TUDelft

Delft University of Technology

A CNN-LSTM Method for the Morphology Evolution Prediction of Beach Mega-Nourishment

Li, Yong; Oosterom, Peter van; Ge, Ying; Zhang, Xiaoxiang; Baart, Fedor

Important note
To cite this publication, please use the final published version (if applicable).
Please check the document version above.

A CNN–LSTM Method for the Morphology Evolution Prediction of Beach Mega-Nourishment

YONG LI[1], PETER VAN OOSTEROM[2], YING GE[1], XIAOXIANG ZHANG[3], AND FEDOR BAART[4]

[1]School of Earth Sciences and Engineering, Hohai University, Nanjing 210098, China
[2]Faculty of Architecture and the Built Environment, GIS Technology Section, Delft University of Technology (TU Delft), 2628 BL Delft, The Netherlands
[3]College of Hydrology and Water Resources, Hohai University, Nanjing 210098, China
[4]Department of Software Data and Innovation, Deltares, 2629 HV Delft, The Netherlands

Corresponding authors: Yong Li (liyong@hhu.edu.cn) and Xiaoxiang Zhang (xiaoxiang@hhu.edu.cn)

ABSTRACT Sand nourishment is widely adopted as an effective soft approach to provide long-term coastal safety, protect the ecology environment, and promote tourism and recreation. With the increase in frequency and expenses in beach nourishment worldwide, an adequate prediction of morphology evolution is greatly desired for coastline management. Based on detailed monitoring data of the mega-nourishment Sand Engine, this article integrates a convolutional neural network (CNN) and long short-term memory (LSTM) to predict the nourishment morphology evolution. The historical surveyed data are transformed into sequence grids, which are input into the CNN to obtain the spatial features of beach nourishment. The CNN is constructed by performing the convolutional and pooling operation on the historical data, which can extract actual spatial features and reduce network complexity. The output of the CNN is input to LSTM to learn the temporal relationship to predict future nourishment terrain using past time-series features. Finally, the LSTM output is decoded by the fully connected layer to obtain the prediction result. The complex spatiotemporal correlations among the input data are identified through effective training of the proposed model. The major contribution of this article is to propose a data-driven model that combines CNN and LSTM for the morphology evolution prediction of beach nourishment, and validate the effectiveness of the proposed model by comparing with the performances of other popular methods in predicting the nourishment changes.

INDEX TERMS Mega-nourishment, long short-term memory, convolutional neural network, nourishment morphology evolution prediction.

NOMENCLATURE

CNN	Convolutional Neural Network
LSTM	Long Short-Term Memory
RNN	Recurrent Neural Network
RTK	Real-Time Kinematic
GPS	Global Positioning System
ReLU	Rectified Linear Unit
MSE	Mean Squared Error
MAE	Mean Absolute Error
RMSE	Root Mean Square Error
IA	Index of Agreement
SVM	Support Vector Machine
BP	Back Propagation

The associate editor coordinating the review of this manuscript and approving it for publication was Waleed M. Alsabhan.

I. INTRODUCTION

Climate change and human-induced factors cause extensive crucial environmental problems such as accelerated sea level rise and increased storm surge, which lead to extensive and frequent flooding and pose a significant threat to low-lying coastal areas [1]. Since coastal regions are usually the most productive urban, commercial, industrial, agricultural, and populated regions around the globe, effective intervention approaches are required to provide long-term sustainable

preservation of safety against the enhanced coastal recession and increased flood risk [1], [2].

Sand nourishment is a soft approach to elevate and widen a beach by placing imported sand along the coast, and this approach has multiple functions including mitigating floods and erosion, protecting the ecological environment, and promoting tourism and recreation [1], [3]. Compared with conventional hard approaches of constructing hard structures such as seawalls and breakwaters, sand nourishment has been considered a more efficient, economical, and environmentally friendly countermeasure that constitutes the first line of coastal protection from sea flood. Moreover, nourishment can boost natural and leisure activities along coastlines because of the creation of additional attractions [4]. Thus, sand nourishment is presently the preferred and widely applied intervention to stabilize coastlines, widen beaches and enhance coastal safety [5], [6]. The volume of sand nourishment around the globe has greatly increased over the last decades, and the nourishment demand is anticipated to increase due to the sea level rise in the coming decades [7]. The Torrey Pines nourishment, which is one of 12 San Diego County sand nourishment projects in 2001, costs $17.5 million [3]. Cardiff, Solana, Imperial Beaches, and five other sites were nourished in 2012 [8]. North San Diego County has designed a 50-year period of continual beach nourishment, which is predicted to cost $160 million [9]. A similar system that combines shore nourishment, beach nourishment, and bypassing is considered in Gold Coast, Australia [10].

Due to the growing costs and frequency of sand nourishment projects worldwide [3] and the gradual increase in size and complexity of nourishments, the morphological evolution prediction of sand nourishment is of major importance [7], [11]. The periodical assessment of nourishment based on measurements plays a crucial role in the necessary adjustments of subsequent nourishment measures and execution [1]. Furthermore, the study on modeling of morphological evolution can provide a guide for the application of sand-related strategies such as mega-nourishment, land reclamation, and artificial islands. However, the detailed monitor data on the nourishment terrain evolution are scarce and previous studies are limited [3], [7], [12].

A mega-nourishment project named ''Sand Engine'' provides a good opportunity to study the nourishment evolution prediction [4]. The Sand Engine is performed as an innovative pilot project to feed adjacent coastal areas and stabilize coastlines in the long-term for sustainable coastline management [4]. The Sand Engine, which has been performed at the Delfland Coast in the Netherlands, used a total volume of 21.5 million m^3 of sand [13]. Since the project initiation phase, the Sand Engine has been well monitored for further studies [2], [5]. The morphology evolution of the Sand Engine has been intensively measured on a monthly basis [1], [5]. However, related studies indicate that the nourishment morphology evolution is influenced by complex and hybrid forcing conditions [14]–[17]. Therefore, the prediction of the dynamic evolution of the Sand Engine is a major

challenge [1]. Since the ultimate terrain development is the accumulated result of various effects, this article focuses on applying data-driven methods to study the nourishment morphological evolution and prediction based on time-series-observed terrain measurements.

The prediction of nourishment morphology evolution belongs to the sequence prediction problem, which inputs historical data and outputs future data. Unlike conventional prediction methods, the deep learning method can employ time-series monitoring data in a prediction model. Hence, spatiotemporal changes from historical data can be considered to obtain predicted data. The deep learning model can reduce the prediction error and achieve optimal performance by gradually training and adjusting [18], [19]. Although deep learning has not been employed in nourishment morphology prediction, deep learning based on spatiotemporal data has become prevalent in many related fields, such as predicting the air pollutant concentration, precipitation distribution, sea level changes, and sea surface temperature [18], [20]–[29].

The recurrent neural network (RNN) has been widely applied in many fields of the sequence prediction problem [22]. The long short-term memory (LSTM) network improves the hidden layer of RNN, which can handle long-term dependence problems and enhance the prediction performance [19], [24]. Thus, the LSTM network has proven to be successful in various applications such as machine translation, video classification, image interpretation, and behavior recognition [30]–[34]. The memory blocks in LSTM are adopted to retrieve and store information over time. Temporal dependencies between time-series frames can be learned by recurrently connected cells in the memory block [22]. LSTM has various frameworks such as stateful LSTM, which is designed to learn time-dependent information of long sequences.

Although LSTM has remarkable performance in processing time dependent information, this type of network ignores the spatial relationship in nourishment terrain data. However, nourishment terrain changes depend on time and have correlation with different spatial locations. The accretion or erosion of nourishment sand is a gradual process, and the result is that the beach extent increases or shrinks, and the coastline moves seaward or landward [4]. The historical data have time-dependent and spatial correlation information to learn to predict nourishment terrain changes. Thus, considering spatial information and temporal relation is necessary. The convolutional neural network (CNN) has a powerful ability to analyze spatial information, which is widely applied in spatial data processing issues such as image classification and recognition [35]–[37]. Since the accretion or erosion of nourishment sand has spatial correlation, using CNN to extract context spatial features is reasonable.

The main objective of this study is to present a data-driven approach that combine CNN and LSTM by fully exploiting the information in temporal and spatial dimensions for the nourishment morphology prediction. The historical surveyed data should be preprocessed and formulated
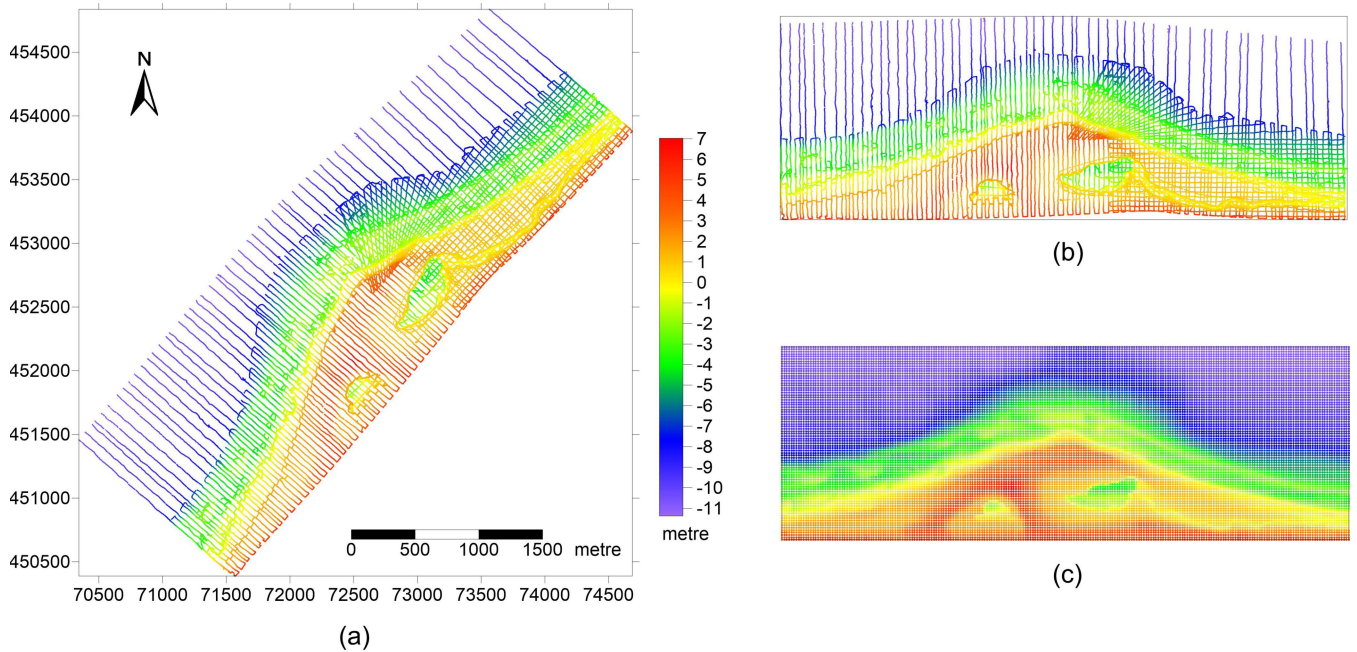
FIGURE 1. Data of the study area.

as the supervised time sequence prediction task. Then, the CNN is employed to learn and derive the specific spatial features of elevation values at different locations in the mega-nourishment. The correlations of accretion or erosion of neighbors on the target location can be reflected by the derived spatial features. The output of CNN is input to LSTM to learn the temporal relationship to predict future nourishment terrain using past time-series features. The complex spatiotemporal correlations among the input data are identified by effectively training the proposed model.

The developed model can be applied for the impact assessment and maintenance of beach mega-nourishments. The mega-nourishments are generally divided into two types: permanent mega-nourishments and feeder-type mega-nourishments [38]. Permanent mega-nourishments are mainly beach extensions, which must be frequently nourished to maintain their size and shape for safety preservation. Feeder-type mega-nourishments freely spread and erode to feed adjacent beaches and dunes with sand. Both types of mega-nourishments require a detailed morphology evolution prediction that can provide insight in the erosion and accretion zones. The morphological prediction results can be applied to determine the nourishment requirements to maintain the size and function of permanent mega-nourishments and assess the details on erosion rates and life span of feeder-type mega-nourishments.

The major contributions of this article are: (1) to the best of our knowledge, the research presented in this article is the first to employ CNN and LSTM for the morphology evolution prediction of beach nourishment; (2 this study validates the effectiveness of the proposed model; (3) this article compares the performances of several popular methods in predicting nourishment changes.

Section II presents the nourishment study data and proposed model combining CNN and LSTM. Section III introduces the qualitative and quantitative experiments and analyzes the experimental results. Finally, Section IV presents the conclusion.

II. DATA AND METHODOLOGY

A. STUDY DATA

The Sand Engine, which is a mega-nourishment project constructed in 2011 in the Netherlands, used 21.5 million m^3 of sand for coastal protection, coastline maintenance, and ecological and recreational purposes [2], [4]. The initial nourishment spanned the coastal area, which has an alongshore length of approximately 2.4 km and a cross-shore width of up to 1 km. As shown in Fig. 1(a), the Sand Engine has a specific shape, which is designed to form an appealing region for nature and recreation [2].

The Sand Engine has been monitored since its completion in the summer of 2011. The Sand Engine morphological evolution is surveyed on a monthly scale using an RTK-GPS and an echo sounder [2]. The surveyed area measures 1.6 km in cross-shore width and 4.7 km in alongshore length. Three days are usually required to perform the monthly surveys of the entire area under calm weather conditions.

To facilitate the display and analysis of terrain changes and the usage of CNN, raw measurement data are rotated to the alongshore direction as depicted in Fig. 1(b). The irregular distributed measurements are transformed to the grids using the inverse distance weighting interpolation as depicted in Fig. 1(c). The grid cell size is 20 m × 20 m.

B. CNN FOR SPATIAL CORRELATION

The spatial correlation of the nourishment terrain can be obtained using the CNN model. A CNN connects neural cells with cells in a local window of the previous layer, which can be used to explore the spatial relationship among nearby locations. The spatial correlation features among long-distance locations can be identified by deep neural layers [34]. CNN has the advantages of spatial arrangement and local connectivity among layer nodes, which enable the architecture to well extract features from the input grids of a sand nourishment terrain. A CNN is mainly composed of two types of layers: convolutional layers and pooling layers. Convolutional layers are employed to extract the spatial features of a nourishment terrain, whereas pooling layers can remarkably enhance the computing efficiency by decreasing the number of links between layers. The same weight is shared by all cells in the same layers, which further relieve the computational burden [25]. The spatial features of a nourishment terrain are exported after convolutional and pooling operations.

The CNN has four types of layers: input, convolutional, pooling, and output layers. The grid data transformed from the nourishment measurements are input to the CNN model. The input and output of convolutional layers are presented as follows [32]:

$$X_l = f(W_l \otimes X_{l-1} + b_l) \qquad (1)$$

where X_l and X_{l-1} are the *lth* and $(l-1)th$ layer matrix; f is the activation function; the weight and bias of *lth* layer are W_l and b_l, respectively. For the convolutional layers in the model, the activation function of rectified linear unit (ReLU) is used as (2).

$$f(x) = \max(0, x) \qquad (2)$$

Spatial information from a mega-nourishment project can be effectively extracted, and the network scale can be reduced by the combination of activation functions and convolutional layers. To further optimize the network structures and enhance the computation efficiency, the pooling layer is added after the convolutional layers to decline the layer dimension. The max pooling function expressed as (3) is applied in the pooling layer of this model.

$$pooling_{max}(X_l) = \max(x_{i,j}|i,j \in D_{pooling}) \qquad (3)$$

where $x_{i,j}$ is the element of layer X_l, and $D_{pooling}$ is the domain of the pooling layer.

The spatial correlation features of a mega-nourishment project acquired from the CNN model are flattened to a highly concentrated one-dimensional vector and placed into the subsequent LSTM model.

C. LSTM FOR SEQUENCE EXPRESSION

Temporal dependency plays another crucial role in the nourishment terrain evolution prediction. The erosion or accretion of nourishment terrain usually has a tendency that can be learned from historical data. Therefore, considering the correlation and influence among the time-series features is necessary for nourishment morphology prediction.

The LSTM network can store long-term dependencies by introducing the structure of memory units, which solve the problems of gradient vanishing or explosion in the recurrent neural network. The storage unit contains three types of gates: input gate, forget gate, and output gate. The input gate is employed to control how the units select new features to store. The forget gate is designed to selectively abandon some past nourishment data information. The output gate is used to determine which information is delivered from memory units. The three gates and memory units are presented as follows [20]:

$$i_t = \sigma(W_i[h_{t-1}, x_t] + b_i) \qquad (4)$$
$$f_t = \sigma(W_f[h_{t-1}, x_t] + b_f) \qquad (5)$$
$$c'_t = \tanh(W_c[h_{t-1}, x_t] + b_t) \qquad (6)$$
$$c_t = f_t \odot c_{t-1} + i_t \odot c'_t \qquad (7)$$
$$o_t = \sigma(W_o[h_{t-1}, x_t] + b_o) \qquad (8)$$
$$h_t = o_t \odot \tanh(c_t) \qquad (9)$$

where x_t is the input at time t; i_t, f_t, and o_t are three types of gates: input, forget, and output gates; h, W, and b are the state of the hidden layer, corresponding weight matrix, and bias, respectively; σ is the sigmoid function; c'_t is the input memory cell; c_t is the output memory cell. The hyperbolic tangent function is represented by the term tanh.

D. NOURISHMENT TERRAIN PREDICTION

The spatial and temporal features are extracted by the CNN and LSTM as shown in Fig. 2. Finally, the output of the LSTM is decoded by the fully connected layer to obtain the prediction result of the nourishment terrain. The framework of the proposed model for nourishment morphology evolution prediction is shown as Fig. 2. The convolution processes in our implementation are performed with a kernel size of 3×3, a stride of 1×1, and the "Same-Padding". Hence, the spatiotemporal features have identical spatial size after the convolution processes. The convolutional layers and LSTM layer exploit the activation function of ReLU.

In addition, stateful LSTM is adopted to achieve the stable long-term prediction of nourishment morphology evolution. To build the relationship in the long time-series sequence, stateful LSTM initializes the state of the sample batch by using the state of the memory cell of the previous batch. Thus, stateful LSTM can maintain the state information over a long sequence, which is suitable for the modeling based on the long time-series data of nourishment [39]. The time lags are set to 3 in this research. The time-series grids are processed by the CNN and stateful LSTM, which enable the spatiotemporal features to have an efficient representation. This proposed architecture is an end-to-end model whose output has identical spatial dimensions to the input grids. Table 1 presents the parameters of the proposed model.
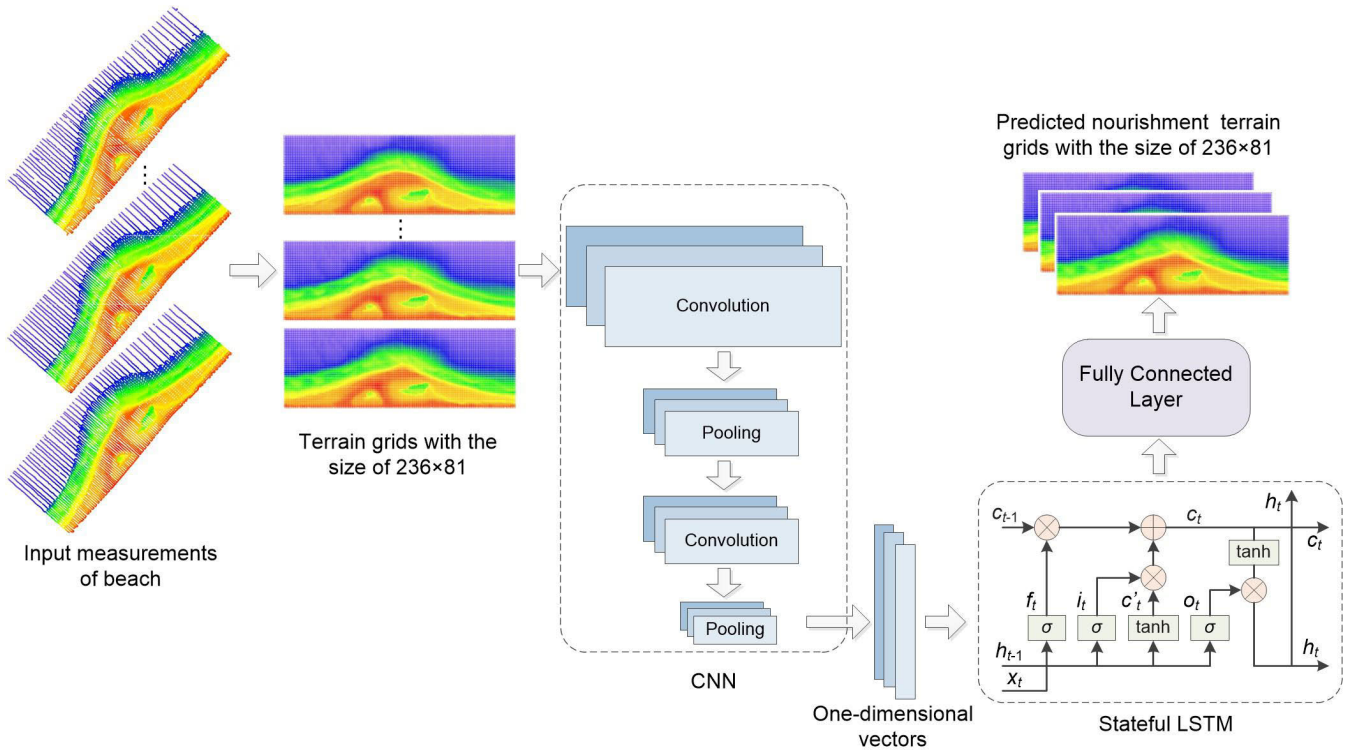
FIGURE 2. Framework of the proposed method to predict the nourishment morphology evolution.

The weights and bias of this model are updated, and the network prediction performance is optimized through the training process as shown by the flowchart in Fig. 3. To minimize the difference between predicted and surveyed terrain grids of nourishment, the mean squared error (MSE) is adopted as the loss function of the model, which can be presented as follows.

$$MSE = \frac{1}{n} \sum_{i=1}^{n} (z'_i - z_i)^2 \qquad (10)$$

where z'_i and z_i are the predicted and surveyed elevation values of nourishment terrain, respectively.

III. EXPERIMENT AND RESULTS

The dataset in this article contain the mega-nourishment terrain data from August 2011 to September 2015, which were collected as described in the above introduction of study data. Thirty-two terrain grids were generated from the time-series measurements of the mega-nourishment. In total, 23 grids in August 2011 to April 2014 were employed as the training set, and 9 grids from July 2014 to September 2015 were used as the test set.

We used the interpolated grids as input to our model. Each input sample consists of three past grid data. The output is a predicted next terrain grid representing elevation values. Thus, the model in this study is a one-step prediction model using past surveying data. The number of training iterations was 30 epochs. To perform multiple-step prediction, the recursive method is used to predict the future

mega-nourishment terrain after the time steps for training. In the recursive prediction process, the predicted values are used as inputs with the last data for the next prediction.

In the experiments, the effectiveness of different prediction methods is evaluated by four evaluation indices including the Mean Absolute Error (MAE), Root Mean Square Error (RMSE), Pearson correlation coefficient and Index of Agreement (IA) as follows:

$$MAE = \frac{1}{n} \sum_{i=1}^{n} |z'_i - z_i| \qquad (11)$$

$$RMSE = \sqrt{\frac{1}{n} \sum_{i=1}^{n} (z'_i - z_i)^2} \qquad (12)$$

$$\rho = \frac{n \sum_{i=1}^{n} z_i z'_i - \sum_{i=1}^{n} z_i \sum_{i=1}^{n} z'_i}{\sqrt{n \sum_{i=1}^{n} z_i^2 - (\sum_{i=1}^{n} z_i)^2} \sqrt{n \sum_{i=1}^{n} z'^2_i - (\sum_{i=1}^{n} z'_i)^2}} \qquad (13)$$

$$IA = 1 - \frac{\sum_{i=1}^{n} (|z'_i - z_i|)^2}{\sum_{i=1}^{n} (|z_i - z| + |z'_i - z|)^2} \qquad (14)$$

where z_i and z'_i are the surveyed and predicted values of the nourishment terrain elevation, respectively; z is the average of z_i; n is the number of grid cells; ρ is Pearson correlation coefficient.
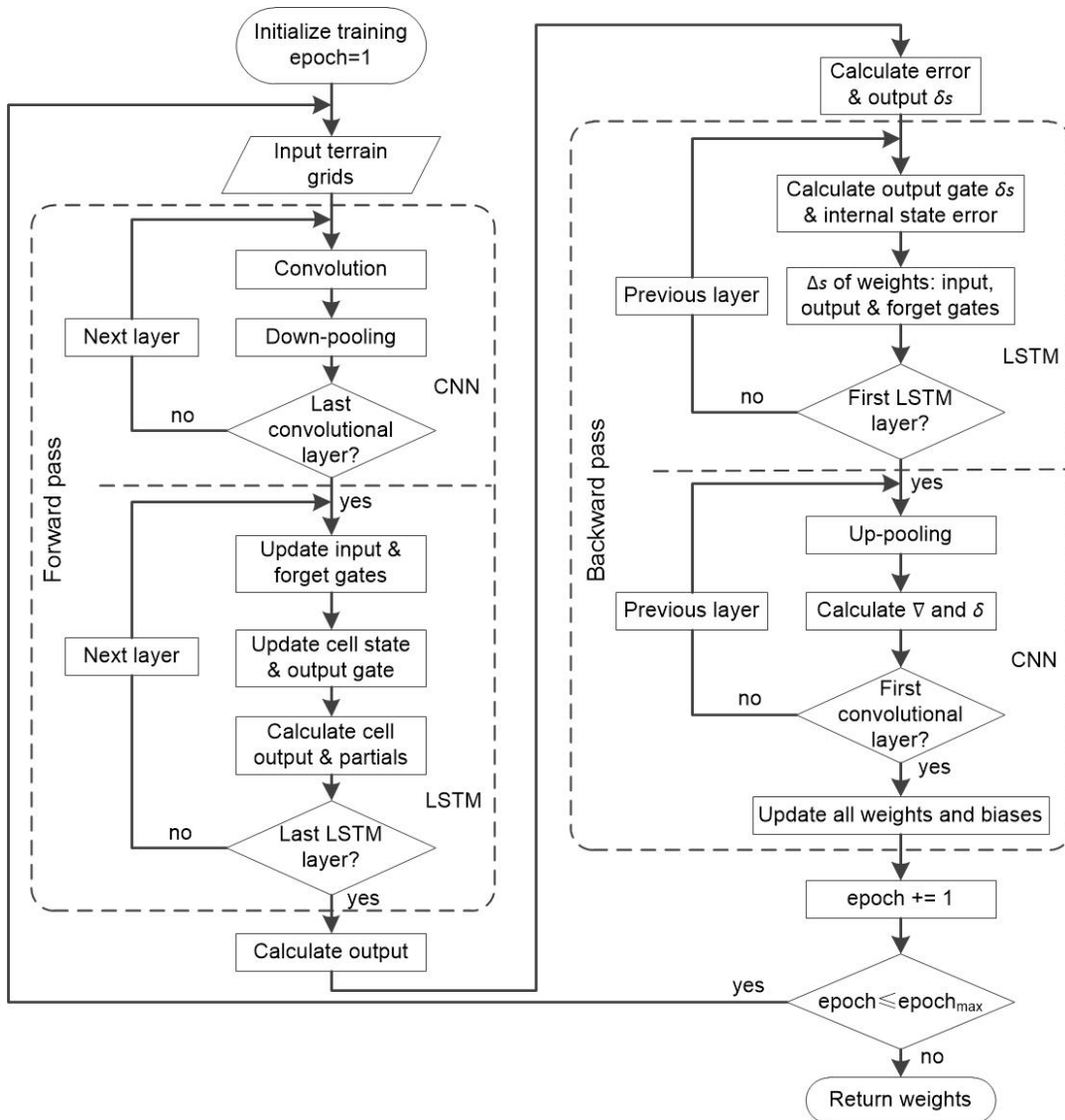
FIGURE 3. Flowchart of the methodology of this article (δ, Δ, s, and ∇ represents the training errors, weight changes, neurons, and gradients, respectively).

Five popular methods are selected for the prediction performance comparison with the proposed model: Support Vector Machine (SVM), Back Propagation (BP) neural network, CNN, RNN, and LSTM. Table 2 presents the parameters for different methods. Each model adopted the recursive prediction process and the same dataset as the proposed model.

Fig. 4-7 shows the variation of four evaluation indices of each model over the prediction time. The recursive method tends to be influenced by error accumulation, so the MAE and RMSE of each model generally increase, and the correlation coefficient and IA values decrease during the recursive prediction. From the statistical results, all of these methods have high Pearson correlation coefficient, which implies that the trend of terrain changes predicted for each time are consistent with the corresponding true terrain. Except for SVM, all methods have relatively low MAE and RMSE and high IA.

The average MAE, RMSE, Pearson correlation coefficient and IA values of the six different models are shown in Figs. 8-11. In terms of Pearson correlation coefficient, all six models are larger than 0.98, which implies that these models have predictability. In terms of MAE, RMSE and IA, the proposed model has the best performance as shown in Figs. 8, 9 and 11. CNN can effectively abstract spatial features, so CNN acquires a slightly lower RMSE than the BP-based method. Compared to the performance of the CNN, the RNN can improve the nourishment terrain change prediction performance because the RNN considers the temporal dependence. In contrast, the LSTM-based method has smaller MAE and RMSE than the RNN-based method at 0.11 and 0.06. This result implies that LSTM can better handle the relationship of long-term sequence. Furthermore, the proposed model, which combines CNN and LSTM, yields better results than LSTM. The results indicate that the pre-
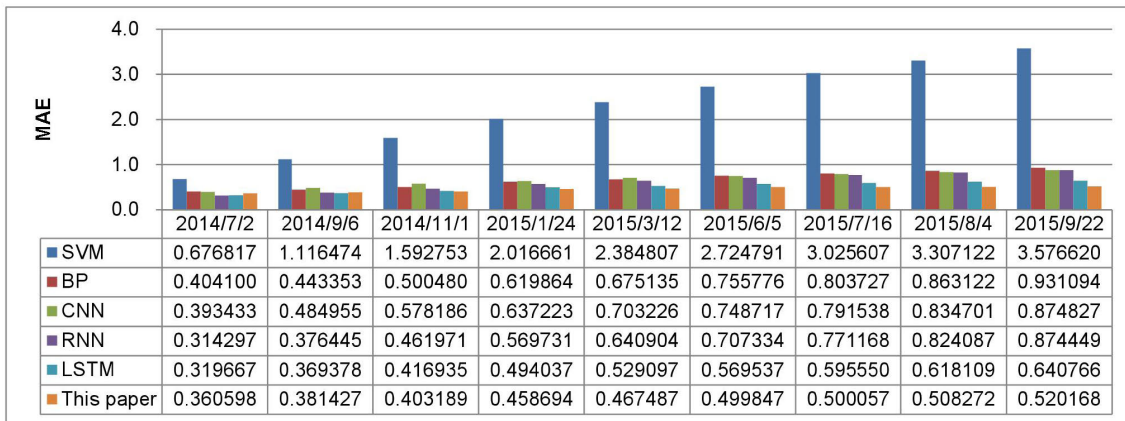
MAE	2014/7/2	2014/9/6	2014/11/1	2015/1/24	2015/3/12	2015/6/5	2015/7/16	2015/8/4	2015/9/22
SVM	0.676817	1.116474	1.592753	2.016661	2.384807	2.724791	3.025607	3.307122	3.576620
BP	0.404100	0.443353	0.500480	0.619864	0.675135	0.755776	0.803727	0.863122	0.931094
CNN	0.393433	0.484955	0.578186	0.637223	0.703226	0.748717	0.791538	0.834701	0.874827
RNN	0.314297	0.376445	0.461971	0.569731	0.640904	0.707334	0.771168	0.824087	0.874449
LSTM	0.319667	0.369378	0.416935	0.494037	0.529097	0.569537	0.595550	0.618109	0.640766
This paper	0.360598	0.381427	0.403189	0.458694	0.467487	0.499847	0.500057	0.508272	0.520168

FIGURE 4. MAE in meters of each model on the prediction over time.

RMSE	2014/7/2	2014/9/6	2014/11/1	2015/1/24	2015/3/12	2015/6/5	2015/7/16	2015/8/4	2015/9/22
SVM	0.756599	1.241663	1.776573	2.255323	2.665828	3.059870	3.409626	3.738954	4.056498
BP	0.707707	0.770533	0.852546	1.013318	1.089875	1.189393	1.254877	1.329928	1.416038
CNN	0.600476	0.701328	0.819328	0.923811	0.993749	1.046300	1.091934	1.142063	1.197288
RNN	0.546303	0.613749	0.704797	0.843241	0.920651	0.995725	1.064594	1.127420	1.197614
LSTM	0.612545	0.663862	0.719075	0.829324	0.865555	0.905371	0.925293	0.944740	0.976307
This paper	0.569097	0.615122	0.658446	0.765988	0.793294	0.835524	0.843881	0.856351	0.878748

FIGURE 5. RMSE in meters of each model on the prediction over time.

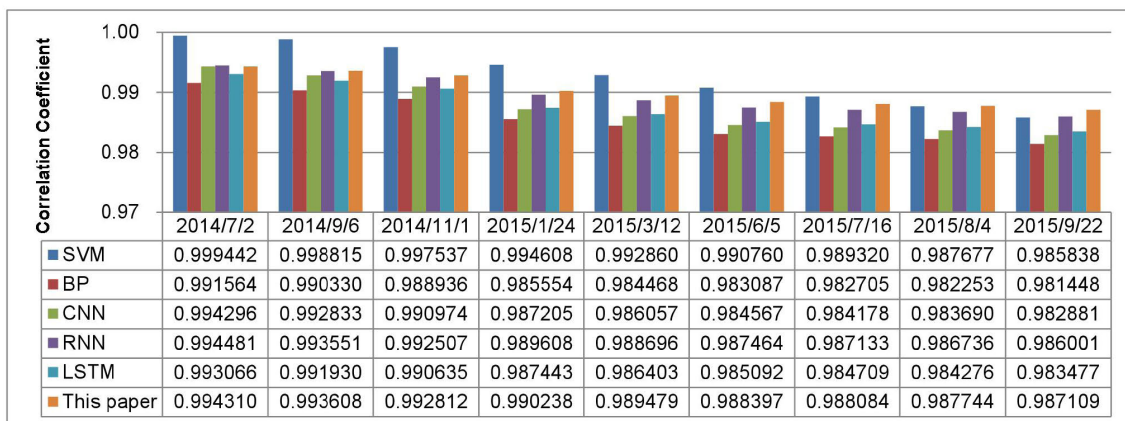| Correlation Coefficient	2014/7/2	2014/9/6	2014/11/1	2015/1/24	2015/3/12	2015/6/5	2015/7/16	2015/8/4	2015/9/22
SVM	0.999442	0.998815	0.997537	0.994608	0.992860	0.990760	0.989320	0.987677	0.985838
BP	0.991564	0.990330	0.988936	0.985554	0.984468	0.983087	0.982705	0.982253	0.981448
CNN	0.994296	0.992833	0.990974	0.987205	0.986057	0.984567	0.984178	0.983690	0.982881
RNN	0.994481	0.993551	0.992507	0.989608	0.988696	0.987464	0.987133	0.986736	0.986001
LSTM	0.993066	0.991930	0.990635	0.987443	0.986403	0.985092	0.984709	0.984276	0.983477
This paper	0.994310	0.993608	0.992812	0.990238	0.989479	0.988397	0.988084	0.987744	0.987109

FIGURE 6. Pearson correlation coefficient of each model on the prediction over time.

diction performance can be improved by adding the CNN to LSTM to consider time-dependent information based on the spatial correlation features of the mega-nourishment terrain. In summary, the proposed method is more suitable for the spatiotemporal sequence prediction of mega-nourishment terrain.

Furthermore, to examine the statistical significance of the improvement of the proposed method, the prediction RMSEs
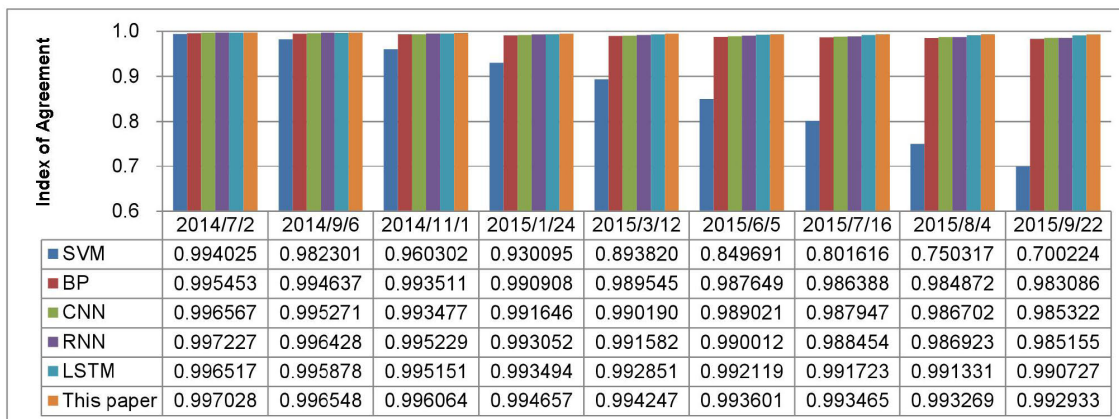
	2014/7/2	2014/9/6	2014/11/1	2015/1/24	2015/3/12	2015/6/5	2015/7/16	2015/8/4	2015/9/22
SVM	0.994025	0.982301	0.960302	0.930095	0.893820	0.849691	0.801616	0.750317	0.700224
BP	0.995453	0.994637	0.993511	0.990908	0.989545	0.987649	0.986388	0.984872	0.983086
CNN	0.996567	0.995271	0.993477	0.991646	0.990190	0.989021	0.987947	0.986702	0.985322
RNN	0.997227	0.996428	0.995229	0.993052	0.991582	0.990012	0.988454	0.986923	0.985155
LSTM	0.996517	0.995878	0.995151	0.993494	0.992851	0.992119	0.991723	0.991331	0.990727
This paper	0.997028	0.996548	0.996064	0.994657	0.994247	0.993601	0.993465	0.993269	0.992933

FIGURE 7. Index of Agreement of each model on the prediction over time.

TABLE 1. Parameters of the proposed model.

Parameters	Value
Number of convolutional layers	2
Kernel size of a convolutional layer	3×3
Number of the first convolutional layer parameters	3×3×16
Number of the second convolutional layer parameters	3×3×8
Number of pooling layers	2
Kernel size of a pooling layer	2×2
Number of the stateful LSTM layers	1
Number of the stateful LSTM nodes	64
Number of fully connected layers	1
Number of fully connected layer nodes	19,116
Training method	Adaptive moment estimation
Batch size	1

TABLE 2. Parameters of the comparison methods.

Models	Parameters
SVM	Radial Basis Function Kernel
BP	2 hidden layers (128 hidden units, 64 hidden units)
CNN	Conv1(3×3×16), pooling1(2×2), Conv2(3×3×8), pooling2(2×2)
RNN	64 hidden units
LSTM	64 hidden units

of those models are statistically compared by conducting the t-test method. The p− values to compare the proposed model with SVM, BP, CNN, RNN and LSTM are 7.66×10^{-4}, 1.71×10^{-4}, 2.67×10^{-4}, 1.04×10^{-2}, and 2.52×10^{-6} ($p<0.05$). The results show that the proposed method can improve the prediction performance.

Different models are performed with Python 3.5.2 and Keras 2.1.6 using a computer with i7-8700 processor, 3.7 GHz CPU, and 16 GB RAM. The average running time of executing SVR, BP, CNN, RNN, LSTM and the proposed model for 30 times is 5.63, 11.29, 183.33, 17.64, 61.92, 46.36 seconds, respectively. The running time of the proposed model is more than that of the SVR, BP and RNN, but less than that of CNN and LSTM. According to the calculation rules of big O notation, the computational complexity of the proposed model is:

$$T = O(\sum_{i=1}^{D} M_i \cdot N_i \cdot K_i^2 \cdot C_{i-1} \cdot C_i)$$
$$+ O(4 \cdot H \cdot (S_{in} + S_{out})) + O(m \cdot n)$$
$$= O(\sum_{i=1}^{D} M_i \cdot N_i \cdot K_i^2 \cdot C_{i-1} \cdot C_i)$$
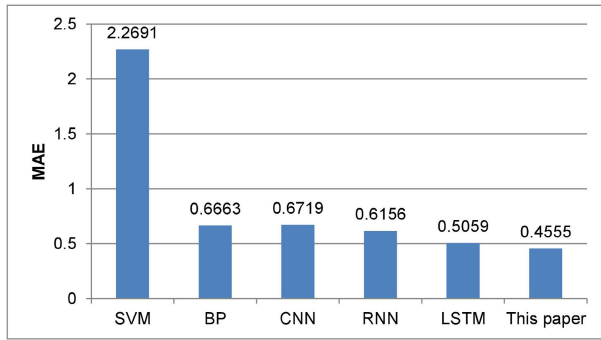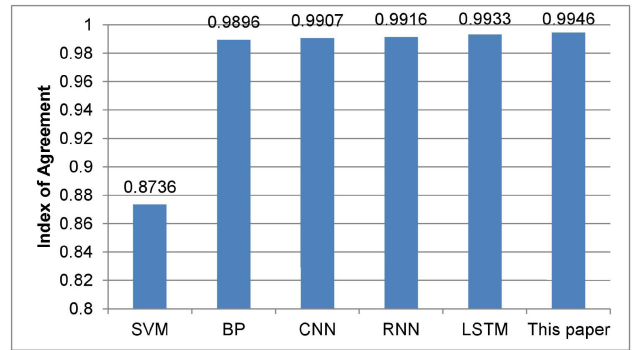$$+ O(H \cdot S_{in} + H^2) + O(m \cdot n) \tag{15}$$

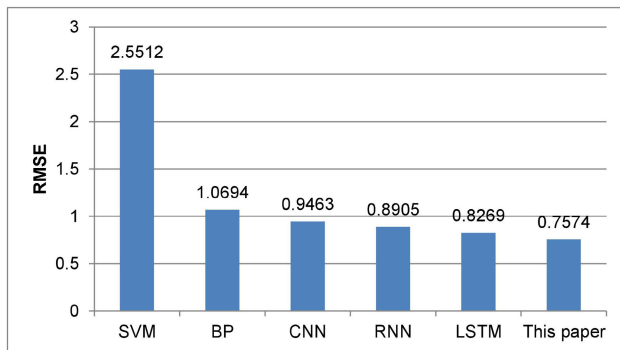**FIGURE 8.** Average MAE in meters of each model on prediction over time.

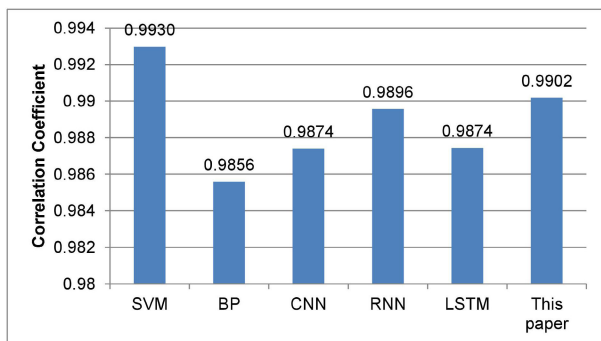**FIGURE 9.** Average RMSE in meters of each model on the prediction over time.

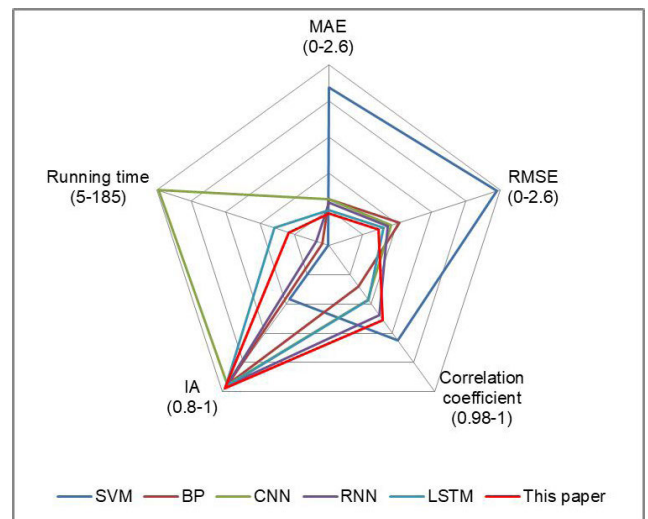**FIGURE 10.** Average Pearson correlation coefficient of each model on the prediction over time.

FIGURE 11. Average IA of each model on prediction over time.

FIGURE 12. Comparison of the average MAE, RMSE, correlation coefficient, IA and running time of different models.

The proposed model has the lowest MAE and RMSE, the second highest correlation coefficient, the highest IA and the fourth smallest running time. Thus, the proposed prediction model has improved the prediction performance compared to the other five prediction models.

Fig. 13, Fig. 14 and Fig. 15 illustrate the observed terrain and predicted results of this proposed model in July 2014, March 2015, and September 2015, respectively. The predicted terrain is generally consistent with the measurements. Relatively large changes are more likely to appear on rugged terrain, which poses greater challenges for the morphology evolution prediction of nourishment. Therefore, the major differences occur at the location with a steep slope.

The Sand Engine Peninsula is the main source of nourishment sand, as denoted by the red polygon in Fig. 16(a). The volume change of the Sand Engine Peninsula is generally calculated to analyze the lifetime of nourishments. The original measured volume of the Sand Engine Peninsula is 16.35 million m^3. The measurements in September 2014 show that a total volume of 2.8 million m^3 has decreased after three years, which is approximately 17% of the original volume.
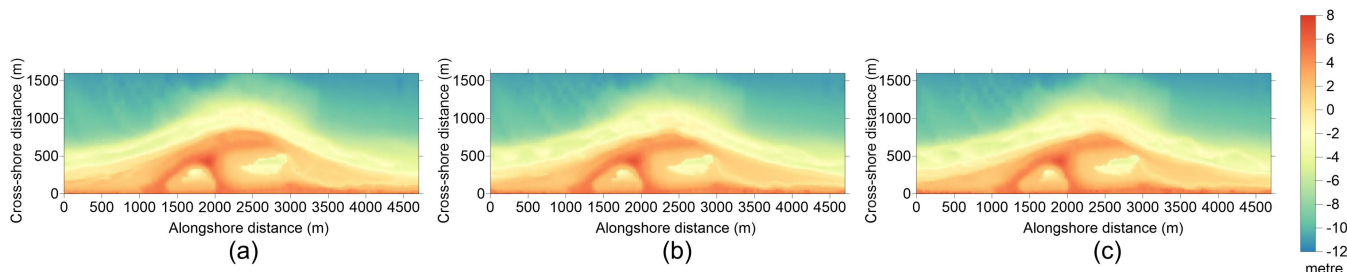
where D is the number of convolutional layers; M and N are the width and height of the feature map derived by each convolutional kernel; K is the size of convolutional kernel; C_{i-1} is the input channels or output channels of the previous layers; C_i is the output channels of the ith layer, which is equal to the number of convolutional kernels; H is the number of LSTM nodes; S_{in} and S_{out} are the input and output sizes of LSTM. Since S_{out} is generally equal to H, the time complexity $O(4 \cdot H \cdot (S_{in} + S_{out}))$ can be simplified as $O(H \cdot S_{in} + H^2)$. m and n are the input and output sizes of the fully connected layer.

The average MAE, RMSE, correlation coefficient, IA and running time of different models are compared in Fig. 12.

FIGURE 13. True terrain values of nourishment. (a–c) Survey periods of the terrains are July 2014, March 2015, and September 2015.
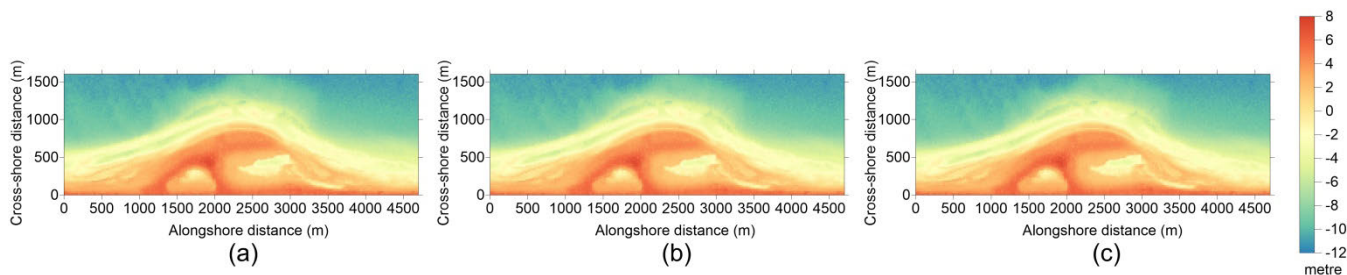

FIGURE 14. Predicted terrain values of nourishment. (a–c) Predicted terrains by July 2014, March 2015, and September 2015.
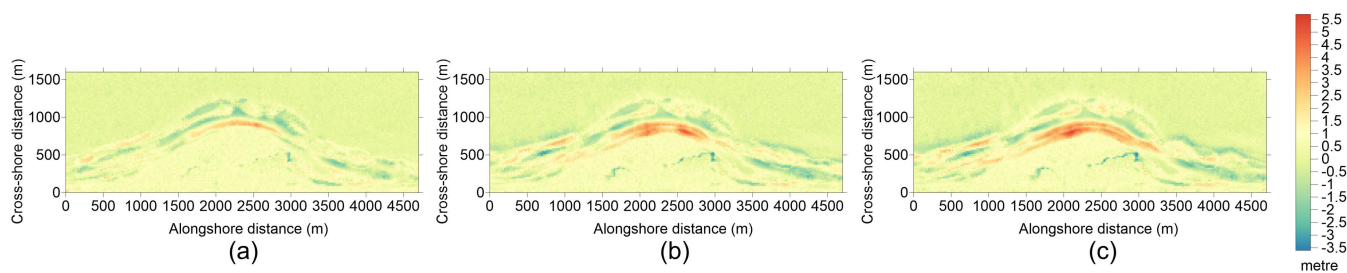

FIGURE 15. Error maps of the nourishment terrain prediction. (a–c) Differences between true terrain and predicted terrain in July 2014, March 2015, and September 2015.
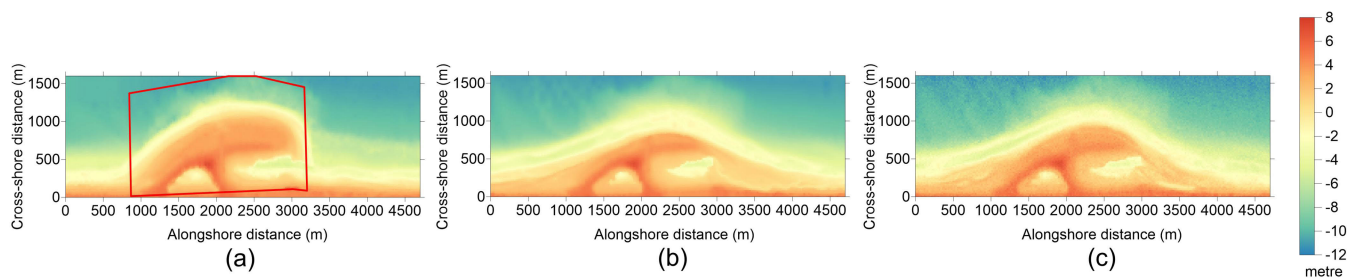

FIGURE 16. Predicted result of nourishment terrain after three years. (a) Original nourishment measurements in August 2011 (The red polygon represents the Sand Engine Peninsula). (b) Nourishment measurements after three years. (c) Result predicted by the proposed model in this article.

Since data on the morphology evolution of mega-nourishments is scarce, previous studies focus on hydrodynamic models. Reference [40] using a standard diffusion type coastline model to calculate the erosion rate of nourishments. Approximately 70% of the original volume of the Sand Engine would decrease after three years according to this model [40]. However, approximately 17% of the volume of the Sand Engine has decreased after 3 years in reality (see Fig. 16).

Reference [38] adopts the numerical model of Delft3D, which is a coastal area model by the advection-diffusion equation and shallow water equations. The Delft3D model is calibrated using the measurement data of the Sand Engine. The result of Delft3D is that the volume erosion is approximately 20% after three years.

These hydrodynamic models are usually based on process formulations considering complex factors such as climate, wave and sediment. The proposed model in this article

predicts the nourishment terrain based on historical data and obtains the result of 12.38% of volume decrease after three years. Compared to the results by the model in [40], the results achieved by reference [38] and ours are more consistent with measurements. Reference [38] overestimates the nourishment volume decrease, while the proposed model underestimates the nourishment volume decrease as shown in Fig. 16.

IV. CONCLUSION

Sand nourishment is a soft approach against environmental problems, such as accelerated sea level rise and increased storm surge. With the increase in frequency and expenses in beach nourishments worldwide, the morphological evolution prediction of sand nourishment is of major importance. To fully exploit the information in spatial and temporal dimensions, a data-driven approach combining CNN and LSTM is constructed to predict the nourishment morphology evolution. The historical surveyed data is transformed into sequence grids, which are input into a CNN to obtain the spatial features of the mega-nourishment. The CNN is performed on the historical data, which can extract actual spatial features and reduce the network complexity. LSTM is used to account for the time dependence of nourishment terrain changes. The output of CNN is input to LSTM to learn the temporal relationship to predict future nourishment terrain using past time-series features. The LSTM output is finally decoded by the fully connected layer to obtain the prediction result. The complex spatiotemporal correlations among the input data are identified by effectively training the proposed model. In comparison with other popular methods, the experimental results conducted on the Sand Engine dataset show that the proposed model improved the prediction of the nourishment morphology evolution.

Improvements can be considered in future studies to better predict the nourishment morphology evolution. The spatiotemporal information of nourishment terrain can be encoded by using various methods such as multimodal learning to obtain effective features. To transform raw measurement data into sequence grids, a more accurate interpolation method can be explored to consider the context along temporal dimension.

ACKNOWLEDGMENT

REFERENCES

[1] C. Brière, S. K. H. Janssen, A. P. Oost, M. Taal, and P. K. Tonnon, "Usability of the climate-resilient nature-based sand motor pilot, The Netherlands," *J. Coastal Conservation*, vol. 22, no. 3, pp. 491–502, Jun. 2018.

[2] M. J. F. Stive, M. A. de Schipper, A. P. Luijendijk, S. G. J. Aarninkhof, C. van Gelder-Maas, J. S. M. van Thiel de Vries, S. de Vries, M. Henriquez, S. Marx, and R. Ranasinghe, "A new alternative to saving our beaches from sea-level rise: The sand engine," *J. Coastal Res.*, vol. 290, pp. 1001–1008, Sep. 2013.

[3] B. C. Ludka, R. T. Guza, and W. C. O'Reilly, "Nourishment evolution and impacts at four southern california beaches: A sand volume analysis," *Coastal Eng.*, vol. 136, pp. 96–105, Jun. 2018.

[4] M. Taal, M. Loffler, C. Vertegaal, J. Wijsman, L. Van der Valk, and P. Tonnon, *Development of Sand Motor: Concise Report Describing the First Four Years of the Monitoring and Evaluation Programme*. Delft, The Netherlands: Deltares, 2016.

[5] M. A. de Schipper, S. de Vries, G. Ruessink, R. C. de Zeeuw, J. Rutten, C. van Gelder-Maas, and M. J. F. Stive, "Initial spreading of a mega feeder nourishment: Observations of the sand engine pilot project," *Coastal Eng.*, vol. 111, pp. 23–38, May 2016.

[6] J. P. Mulder and P. K. Tonnon, "Sand Engine': Background design a mega-nourishment pilot Netherlands," in *Proc. Conf. Coastal Eng.*, 2011, pp. 3805–3814.

[7] A. P. Luijendijk, R. Ranasinghe, M. A. de Schipper, B. A. Huisman, C. M. Swinkels, D. J. R. Walstra, and M. J. F. Stive, "The initial morphological response of the sand engine: A process-based modelling study," *Coastal Eng.*, vol. 119, pp. 1–14, Jan. 2017.

[8] G. Griggs and N. Kinsman, "Beach widths, cliff slopes, and artificial nourishment along the California coast," *Shore Beach*, vol. 84, no. 1, pp. 3–14, 2016.

[9] P. Diehl, "Solana Beach, Encinitas OK sand replenishment," San Diego Union Tribune, San Diego, CA, USA, Oct. 2015.

[10] B. Castelle, I. L. Turner, X. Bertin, and R. Tomlinson, "Beach nourishments at coolangatta bay over the period 1987–2005: Impacts and lessons," *Coastal Eng.*, vol. 56, no. 9, pp. 940–950, Sep. 2009.

[11] M. A. Davidson, I. L. Turner, K. D. Splinter, and M. D. Harley, "Annual prediction of shoreline erosion and subsequent recovery," *Coastal Eng.*, vol. 130, pp. 14–25, Dec. 2017.

[12] S. M. Arens, J. P. M. Mulder, Q. L. Slings, L. H. W. T. Geelen, and P. Damsma, "Dynamic dune management, integrating objectives of nature development and coastal safety: Examples from The Netherlands," *Geomorphology*, vol. 199, pp. 205–213, Oct. 2013.

[13] A. Oost, A. C. V. D. Lelij, M. D. Bel, G. O. Essink, and M. Loffler, *The Usability of the Sand Motor Concept*. Delft, The Netherlands: Deltares, 2016.

[14] J. W. Fiedler, P. B. Smit, K. L. Brodie, J. McNinch, and R. T. Guza, "Numerical modeling of wave runup on steep and mildly sloping natural beaches," *Coastal Eng.*, vol. 131, pp. 106–113, Jan. 2018.

[15] O. Burvingt, G. Masselink, P. Russell, and T. Scott, "Classification of beach response to extreme storms," *Geomorphology*, vol. 295, pp. 722–737, Oct. 2017.

[16] G. Coco, N. Senechal, A. Rejas, K. R. Bryan, S. Capo, J. P. Parisot, J. A. Brown, and J. H. M. Macmahan, "Beach response to a sequence of extreme storms," *Geomorphology*, vol. 204, pp. 493–501, Jan. 2014.

[17] R. A. Morton and A. H. Sallenger, Jr., "Morphological impacts of extreme storms on sandy beaches and barriers," *J. Coastal Res.*, vol. 19, pp. 560–573, 2003.

[18] D. Qin, J. Yu, G. Zou, R. Yong, Q. Zhao, and B. Zhang, "A novel combined prediction scheme based on CNN and LSTM for urban PM2.5 concentration," *IEEE Access*, vol. 7, pp. 20050–20059, 2019.

[19] T. J. Sejnowski, *The Deep Learning Revolution*. Cambridge, MA, USA: MIT Press, 2018.

[20] C. Wen, S. Liu, X. Yao, L. Peng, X. Li, Y. Hu, and T. Chi, "A novel spatiotemporal convolutional long short-term neural network for air pollution prediction," *Sci. Total Environ.*, vol. 654, pp. 1091–1099, Mar. 2019.

[21] C. Ma, S. Li, A. Wang, J. Yang, and G. Chen, "Altimeter observation-based eddy nowcasting using an improved Conv-LSTM network," *Remote Sens.*, vol. 11, pp. 783–800, Jan. 2019.

[22] Y. Yang, J. Dong, X. Sun, E. Lima, Q. Mu, and X. Wang, "A CFCC-LSTM model for sea surface temperature prediction," *IEEE Geosci. Remote Sens. Lett.*, vol. 15, no. 2, pp. 207–211, Feb. 2018.

[23] S. Xingjian, Z. Chen, H. Wang, D.-Y. Yeung, W.-K. Wong, and W.-C. Woo, "Convolutional LSTM network: A machine learning approach for precipitation nowcasting," in *Proc. Adv. Neural Inf. Process. Syst.*, 2015, pp. 802–810.

[24] C. Huang and P. Kuo, "A deep CNN-LSTM model for particulate matter (PM2. 5) forecasting in smart cities," *Sensors*, vol. 18, pp. 2220–2242, Jul. 2018.

[25] N. K. Kumar, R. Savitha, and A. A. Mamun, "Regional ocean wave height prediction using sequential learning neural networks," *Ocean Eng.*, vol. 129, pp. 605–612, Jan. 2017.

[26] Z. Yang, W. Jiang, B. Xu, Q. Zhu, S. Jiang, and W. Huang, "A convolutional neural network-based 3D semantic labeling method for ALS point clouds," *Remote Sens.*, vol. 9, no. 9, p. 936, Sep. 2017.

[27] E. Shelhamer, J. Long, and T. Darrell, "Fully convolutional networks for semantic segmentation," *IEEE Trans. Pattern Anal. Mach. Intell.*, vol. 39, no. 4, pp. 640–651, Apr. 2017.

[28] Q. Liu, F. Zhou, R. Hang, and X. Yuan, "Bidirectional-convolutional LSTM based spectral-spatial feature learning for hyperspectral image classification," *Remote Sens.*, vol. 9, no. 12, p. 1330, Dec. 2017.

[29] S. H. Khan, X. He, F. Porikli, and M. Bennamoun, "Forest change detection in incomplete satellite images with deep neural networks," *IEEE Trans. Geosci. Remote Sens.*, vol. 55, no. 9, pp. 5407–5423, Sep. 2017.

[30] D. Ouyang, Y. Zhang, and J. Shao, "Video-based person re-identification via spatio-temporal attentional and two-stream fusion convolutional networks," *Pattern Recognit. Lett.*, vol. 117, pp. 153–160, Jan. 2019.

[31] G. Zhu, L. Zhang, P. Shen, J. Song, S. A. A. Shah, and M. Bennamoun, "Continuous gesture segmentation and recognition using 3DCNN and convolutional LSTM," *IEEE Trans. Multimedia*, vol. 21, no. 4, pp. 1011–1021, Apr. 2019.

[32] X. Ma, J. Zhang, B. Du, C. Ding, and L. Sun, "Parallel architecture of convolutional bi-directional LSTM neural networks for network-wide metro ridership prediction," *IEEE Trans. Intell. Transp. Syst.*, vol. 20, no. 6, pp. 2278–2288, Jun. 2019.

[33] A. Ullah, J. Ahmad, K. Muhammad, M. Sajjad, and S. W. Baik, "Action recognition in video sequences using deep bi-directional LSTM with CNN features," *IEEE Access*, vol. 6, pp. 1155–1166, 2018.

[34] F. Karim, S. Majumdar, H. Darabi, and S. Chen, "LSTM fully convolutional networks for time series classification," *IEEE Access*, vol. 6, pp. 1662–1669, 2018.

[35] D. Balderas, P. Ponce, and A. Molina, "Convolutional long short term memory deep neural networks for image sequence prediction," *Expert Syst. Appl.*, vol. 122, pp. 152–162, May 2019.

[36] N. Lu, Y. Wu, L. Feng, and J. Song, "Deep learning for fall detection: Three-dimensional CNN combined with LSTM on video kinematic data," *IEEE J. Biomed. Health Informat.*, vol. 23, no. 1, pp. 314–323, Jan. 2019.

[37] G. Zhu, L. Zhang, P. Shen, and J. Song, "Multimodal gesture recognition using 3-D convolution and convolutional LSTM," *IEEE Access*, vol. 5, pp. 4517–4524, 2017.

[38] P. K. Tonnon, B. J. A. Huisman, G. N. Stam, and L. C. van Rijn, "Numerical modelling of erosion rates, life span and maintenance volumes of mega nourishments," *Coastal Eng.*, vol. 131, pp. 51–69, Jan. 2018.

[39] S. Gupta and D. A. Dinesh, "Resource usage prediction of cloud workloads using deep bidirectional long short term memory networks," in *Proc. IEEE Int. Conf. Adv. Netw. Telecommun. Syst. (ANTS)*, Bhubaneswar, India, Dec. 2017, pp. 1–6.

[40] R. G. Dean and C. Yoo, "Beach-nourishment performance predictions," *J. Waterway Port Coastal Ocean Engineering-asce*, vol. 118, pp. 567–586, Nov. 1992.

PETER VAN OOSTEROM received the M.Sc. degree in technical computer science from the Delft University of Technology, The Netherlands, in 1985, and the Ph.D. degree from Leiden University, in 1990. From 1985 to 1995, he worked with the TNO-FEL Laboratory, The Hague. From 1995 to 2000, he was a Senior Information Manager with the Dutch Cadastre, where he was involved in the renewal of the Cadastral (Geographic) database. Since 2000, he has been a Professor with the Delft University of Technology and the Head of the Section 'GIS Technology.'

YING GE received the B.A. degree in computer science from Wuhan University and the Ph.D. degree in GIS from Nanjing University, China. She has taught courses in GIS and Engineering, Spatial Data Analysis, and Digital Earth. As a Visiting Scholar, she was with the University of Toronto in 2002, 2007, and 2012. Her research interests include application of cloud computing for GIS, big data mining, data parallel computing, and GIS software engineering.

XIAOXIANG ZHANG received the B.S. degree from the School of Remote Sensing and Information Engineering, Wuhan University, Wuhan, China, in 2000, and the Ph.D. degree in geography from Nanjing University, in 2006. He is currently an Associate Professor with the College of Hydrology and Water Resources, Hohai University, Nanjing, China. His research interests include GIS-based spatial analysis and modeling, and costal remote sensing.

YONG LI received the B.S. and M.S. degrees from the School of Remote Sensing and Information Engineering, Wuhan University, Wuhan, China, in 2003 and 2006, respectively, and the Ph.D. degree from the State Key Laboratory of Information Engineering in Surveying, Mapping, and Remote Sensing, Wuhan University, in 2010. He is currently an Associate Professor with the School of Earth Sciences and Engineering, Hohai University, Nanjing, China. His research interests include point cloud data processing, spatiotemporal beach nourishment data analysis, and machine learning.

FEDOR BAART is currently a Specialist with Deltares, The Netherlands. He is an Expert in the field of integrated modeling. He plays a key role as a Software Architect and Developer with Deltares. His research interests include computer models data driven, interactive, visual attractive, and exploratory.

• • •